

See discussions, stats, and author profiles for this publication at: <https://www.researchgate.net/publication/231709668>

# Average Propagation Rate Coefficients in the Free-Radical Copolymerization of Styrene and $\alpha$ -Methylstyrene Measured by Pulsed-Laser Polymerization

ARTICLE in *MACROMOLECULES* · AUGUST 1998

Impact Factor: 5.8 · DOI: 10.1021/ma980028j

---

CITATIONS

33

---

READS

153

## 2 AUTHORS:



Dax Kukulj

31 PUBLICATIONS 1,299 CITATIONS

SEE PROFILE



Thomas P Davis

Monash University (Australia)

498 PUBLICATIONS 19,751 CITATIONS

SEE PROFILE

# Average Propagation Rate Coefficients in the Free-Radical Copolymerization of Styrene and $\alpha$ -Methylstyrene Measured by Pulsed-Laser Polymerization

Dax Kukulj<sup>†</sup> and Thomas P. Davis\*

School of Chemical Engineering and Industrial Chemistry, University of New South Wales, Sydney, NSW 2052, Australia

Received January 8, 1998; Revised Manuscript Received June 10, 1998

**ABSTRACT:** The average propagation rate coefficient,  $\langle k_p \rangle$ , has been measured in the free-radical copolymerization of styrene (STY) and  $\alpha$ -methylstyrene (AMS) using pulsed-laser polymerization. The value of  $\langle k_p \rangle$  was found to decrease by 2 orders of magnitude as the mole fraction of STY,  $f_{\text{STY}}$ , is decreased from 1.00 to 0.12. The effect of temperature on  $\langle k_p \rangle$  was measured over the range 17.9–47.4 °C, and the Arrhenius parameters were determined. The reduction in  $\langle k_p \rangle$  with decreasing  $f_{\text{STY}}$  is primarily attributed to entropic factors associated with the  $\alpha$ -methyl group in AMS, as revealed by a reduction in the Arrhenius preexponential factor,  $A$ . Homopolymerizations of AMS did not yield molecular weight distributions suitable for successful evaluation of  $k_p$  which is attributed to transfer to monomer dominating the chain stopping events. Mathematical expressions relating  $\langle k_p \rangle$  to monomer composition, allowing for different depropagation kinetics, are derived. It was found that depropagation events did not play a significant role in this work and that the terminal model for  $\langle k_p \rangle$  provided an adequate description of the observed propagation kinetics. Since  $k_p$  for pure AMS could not be measured directly, values were estimated by extrapolation of the copolymerization  $\langle k_p \rangle$  data and the resulting Arrhenius parameters are  $E_a = 36.7$  kJ·mol<sup>-1</sup> and  $A = 10^{6.17}$  dm<sup>3</sup>·mol<sup>-1</sup>·s<sup>-1</sup>.

## Introduction

The use of  $\alpha$ -methylstyrene (AMS) as a comonomer in free radical co- and terpolymerizations is widely practiced in the surface coatings industry. AMS can be used to modify the kinetics of copolymerization reactions by sharply reducing the rate of polymerization at relatively low concentrations in the feed. The primary advantage associated with this rate modification is that transfer to monomer becomes a favored chain stopping event<sup>1</sup> and low molecular weight polymers can be manufactured without the requirement for large quantities of chain transfer agents or initiator. The low ceiling temperature of AMS<sup>2,3</sup> also allows an additional control strategy to be employed; as the reaction temperature approaches the ceiling temperature, effects from depropagation become important and so the propagation rate is further decreased and hence the probability of transfer is increased. Thus a range of reaction conditions can be utilized (temperature, monomer concentration, and functional comonomers) to manufacture oligomers. Despite the commercial importance of AMS in polymerization reactions, there has been a dearth of kinetic studies on quantifying its propagation and transfer behavior in copolymerizations. This may be attributed to the difficulty associated with the measurement of the average propagation rate coefficient,  $\langle k_p \rangle$ , by early techniques such as the rotating sector method and a general belief that the poor polymerizability of AMS restricts its utility in polymerization reactions. To date, the majority of studies on AMS copolymerization have centered around investigating the effect of the depropagation reaction on the average copolymer composition (i.e. measuring monomer reactivity ratios),<sup>4–8</sup>

the average rate of copolymerization,<sup>9,10</sup> and the copolymer molecular weights.<sup>10,11</sup>

The aim of the work reported in this paper is to measure the average propagation rate coefficient,  $\langle k_p \rangle$ , in the copolymerization of AMS with styrene (STY) over a range of temperatures using the PLP/MWD technique<sup>12</sup> (based on the analysis of the molecular weight distribution (MWD) of a polymer produced by pulsed-laser polymerization (PLP)). This technique has been used extensively for the determination of propagation rate coefficients in homo- and copolymerizations, and has been recommended by an IUPAC working party.<sup>13,14</sup> In addition, several copolymerization models are compared in their ability to describe the experimental data, viz. terminal, penultimate, and two depropagation models. The results of this work are also used to shed light on why depropagation in AMS is significant at normal reaction temperatures.

## Experimental Section

**Materials.** Styrene (STY) (Aldrich, 99%) and  $\alpha$ -methylstyrene (AMS) (Aldrich, 99%) were purified by passing through a column of activated basic alumina to remove inhibitor. The photoinitiator, benzoin, was purified by recrystallization from methanol. Reactions were prepared in 4 mL Pyrex flasks sealed with rubber septa. The appropriate amounts of STY, AMS, and benzoin were added to the flask prior to deoxygenation by purging with argon.

**Pulsed-Laser Polymerization.** The experimental setup employed for laser initiation was similar to the design described by Davis et al.<sup>15</sup> A Spectra Physics Quanta-Ray DCR-11 pulsed Nd:YAG laser with a HG-2 harmonic generator was used to generate 355 nm laser radiation. The laser pulse energy was tuned to 35 mJ per pulse and was directed vertically through the solutions. The reaction temperature was controlled using a thermostated cell holder, and conversions were maintained below 5%. The polymer was isolated by evaporating off the residual monomer: initially in a fume

\* Author for correspondence.

<sup>†</sup> Present address: Department of Chemistry, University of Warwick, Coventry CV4 7AL, U.K.

cupboard to remove the bulk of the liquid and then in a vacuum oven.

**Size Exclusion Chromatography.** The molecular weight distributions generated by PLP were measured by size exclusion chromatography (SEC) on a modular system, comprising an autoinjector, guard column, two mixed bed columns (60 cm mixed C, and 30 cm mixed E, Polymer Laboratories), and a differential refractive index detector. The eluent was tetrahydrofuran at 1 mL·min<sup>-1</sup> and the system was calibrated with poly(STY) standards ( $2.89 \times 10^6$  to  $1.25 \times 10^3$  g·mol<sup>-1</sup>) and poly(AMS) standards ( $1.25 \times 10^6$  to  $3.5 \times 10^3$  g·mol<sup>-1</sup>) from Polymer Laboratories.

## Results and Discussion

**PLP Experimental Data.** In the PLP/MWD experiment, the average propagation rate coefficient,  $\langle k_p \rangle$ , is calculated from the degree of polymerization of the inflection point,  $\nu$ , on the low molecular weight side of the molecular weight distribution via the following equations:

$$\langle k_p \rangle = \frac{\nu}{[M]_{co} t_f} \quad (1)$$

$$\nu = \frac{M_{inf}}{m_{co}} \quad (2)$$

$$m_{co} = F_{AMS} m_{AMS} + F_{STY} m_{STY} \quad (3)$$

$$[M]_{co} = \frac{1000}{\frac{f_{AMS} m_{AMS}}{d_{AMS}} + \frac{f_{STY} m_{STY}}{d_{STY}}} \quad (4)$$

Here  $M_{inf}$  is the inflection point molecular weight,  $m_{co}$  is the average molecular weight of the repeat unit in the copolymer,  $m_{AMS}$  and  $m_{STY}$  are the molecular weights of AMS (118.18 g·mol<sup>-1</sup>) and STY (104.15 g·mol<sup>-1</sup>), respectively,  $F_{AMS}$  and  $F_{STY}$  are the fractions of AMS and STY in the copolymer, respectively (calculated using the terminal model for composition),  $[M]_{co}$  is the bulk monomer concentration in the comonomer solution,  $f_{AMS}$  and  $f_{STY}$  are the mole fractions of AMS and STY in the comonomer solution, respectively, and  $d_{AMS}$  and  $d_{STY}$  are the densities of AMS and STY in the comonomer solution, respectively (assuming ideal mixing). The monomer densities for styrene were taken from Coulter et al.<sup>16</sup> and fitted by a linear regression giving  $d_{STY}/(\text{g} \cdot \text{cm}^{-3}) = 0.9237 - 8.915 \times 10^{-4} T/^\circ\text{C}$ . The same dependence of density on temperature was assumed for AMS since the reported densities for STY and AMS at 20 °C are virtually identical<sup>16,17</sup> (0.906 and 0.908 g·cm<sup>-3</sup>, respectively).

The accuracy and precision of  $\langle k_p \rangle$  obtained from PLP/MWD experiments is largely governed by the calibration of SEC. This can become a major problem, especially for copolymer samples. Previously, for the copolymerization of STY and methyl methacrylate (MMA), Davis et al.<sup>18</sup> used a weighted average of the homopolymer calibration curves. This approach attracted some criticism but was subsequently fully justified by a comprehensive molecular weight study.<sup>19</sup> In this work, the calibration curves for poly(AMS) and poly(STY) were found to overlay, as shown in Figure 1, and therefore the PLP molecular weight distributions of the copolymers were all analyzed using a poly(STY) calibration. This approach needs to be used with caution since it has been shown that, in some instances, e.g., the

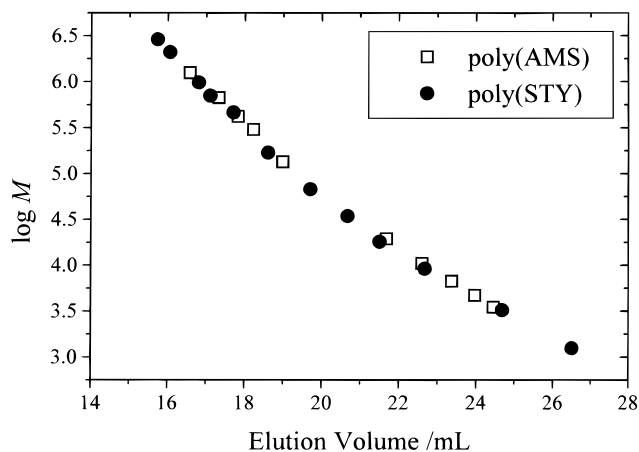


**Figure 1.** Comparison of SEC calibration curves for poly(AMS) and poly(STY). The curves overlay, indicating that poly(AMS) and poly(STY) have very similar hydrodynamic volumes in solution for the same molecular weight.

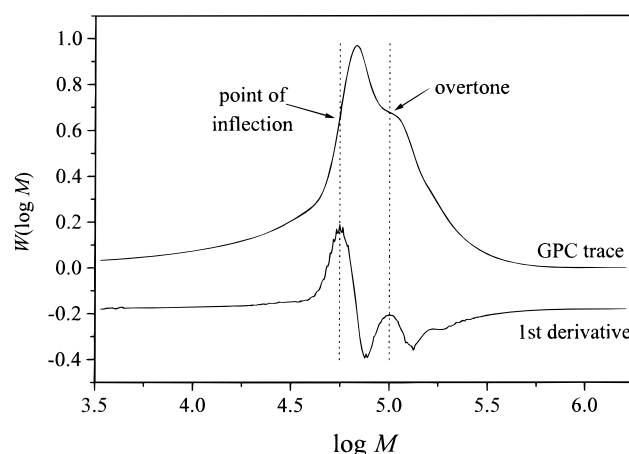


**Figure 2.** Molecular weight distribution,  $W(\log M)$ , and first derivative from pulsed-laser polymerization of styrene at 47.4 °C,  $t_f = 0.25$  s. Note the point of inflection and an overtone at twice the molecular weight.

copolymerization of methyl methacrylate/*n*-butyl acrylate,<sup>20</sup> even if the intrinsic viscosities of the homopolymers are similar, the intrinsic viscosity of the copolymers can be significantly different. For the copolymerization of AMS and STY, however, it has been shown that intrinsic viscosities of the copolymers are very close to those of both the homopolymers,<sup>11</sup> and so analyzing all of the molecular weight distributions against a poly(STY) calibration is justified.

Two examples of molecular weight distributions generated by the PLP experiments are shown in Figures 2 and 3. Figure 2 shows an “ideal” PLP molecular weight distribution displaying clear characteristics of pulsed-laser control over chain initiation and termination processes,<sup>13</sup> i.e., a low molecular weight inflection point (used to calculate  $k_p$ ) and an overtone (at twice the molecular weight of the inflection point). As the fraction of AMS in the comonomer feed is increased ( $f_{STY}$  approaching 0), the PLP characteristics of the experimental molecular weight distributions are less well-defined. The distribution shown in Figure 3 is the worst case example obtained using a comonomer feed,  $f_{AMS} = 0.779$ . Despite the absence of characteristic PLP shape, the inflection point did yield consistent  $\langle k_p \rangle$  numbers at two different pulsing frequencies, and the data were used in the subsequent kinetic analysis. All of the

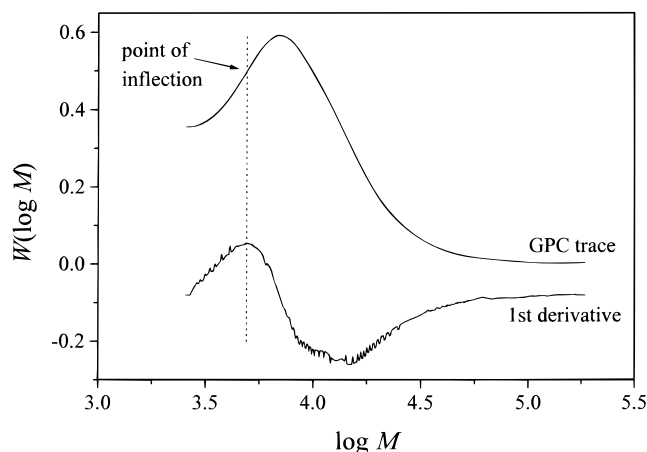


**Figure 3.** Molecular weight distribution,  $W(\log M)$ , and first derivative from pulsed-laser copolymerization of AMS and STY ( $f_{\text{AMS}} = 0.779$ ) at 27.7 °C,  $t_f = 3$  s. The maximum in the derivative is broader than in Figure 2, and there is no overtone.

inflection points were measured from the maximum in the first derivative of the  $W(\log M)$  molecular weight distribution. It is noted that in PLP/MWD analysis it is more common to measure the inflection point from the maximum in the first derivative of the number distribution;<sup>12,21</sup> however, in this work, it was found that this maximum is lost at higher  $f_{\text{AMS}}$ .

The pulsed-laser polymerization of AMS and STY was performed over the temperature range 17.9–47.4 °C. All the data satisfy some of the IUPAC recommended consistency checks,<sup>13</sup> i.e., that the calculated  $\langle k_p \rangle$ s are independent of pulsing rate (at least two pulsing rates were used for each composition) and, in addition, that about half the samples had overtones at twice the molecular weight of the first inflection point (the overtone is lost at higher  $f_{\text{AMS}}$  compositions).

The  $k_p$  for pure AMS could not be measured as appropriate reaction conditions to give characteristic PLP behavior were not found; i.e., the inflection points were not clearly resolvable, and the calculated  $k_p$ s were not independent of pulsing rate. This may be explained by the very high chain transfer to monomer constant for AMS which has been measured to be  $C_S = 4.12 \times 10^{-3}$  at 50 °C;<sup>1</sup> this is approximately 2 orders of magnitude higher than that for STY ( $C_S = 5.27 \times 10^{-5}$  at 50 °C<sup>1</sup>). Therefore chain stopping behavior in PLP is dominated by transfer, rather than by the intermittent irradiation. This explanation also accounts for the loss of secondary peaks in the molecular weight distributions as the AMS concentration in the feed of the copolymerizations is increased.

The measured  $\langle k_p \rangle$  values, plotted on a log scale, appear to vary almost linearly with  $f_{\text{AMS}}$ , as shown in Figure 4. Therefore, an attempt was made to estimate a value of  $k_p$  for AMS on the basis of linear extrapolation. This procedure was adopted for each dataset at the different temperatures. These empirical values of  $k_p$  for AMS are shown in Table 1, alongside those measured for styrene. Since AMS has a significant depropagation rate, the extrapolated values of  $k_p$  for AMS may represent the effective  $k_p$  and not the true value; however, it is shown in a later section that the extrapolated values actually best reflect the true  $k_p$  of AMS. The  $k_p$  values for AMS are lower than the  $k_p$ s for STY by a factor of approximately 170. This reduction is consistent with the trends observed for similar monomer pairs, e.g., at 30 °C, butyl methacrylate:<sup>22</sup>butyl

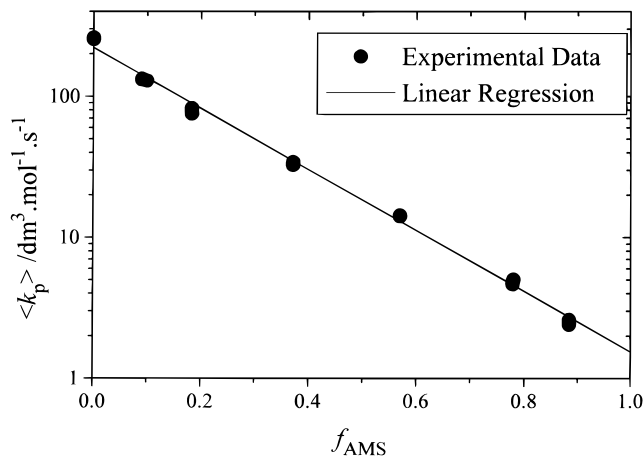


**Figure 4.** Dependence of  $\log \langle k_p \rangle$  on  $f_{\text{AMS}}$  measured by PLP at 47.4 °C. The solid line is the linear regression used to estimate the value for  $k_p^{\text{AMS}}$ .

**Table 1.** Values of  $k_p^{\text{AMS}}$  Obtained from Linear Extrapolation of  $\log \langle k_p \rangle$  vs  $f_{\text{AMS}}$  Data and Average of Measured  $k_p^{\text{STY}}$  Values

$T/^\circ\text{C}$	$k_p^{\text{AMS}}/\text{dm}^3\cdot\text{mol}^{-1}\cdot\text{s}^{-1}$	$k_p^{\text{STY}}/\text{dm}^3\cdot\text{mol}^{-1}\cdot\text{s}^{-1}$
47.4	1.54	257
37.6	1.03	160
27.7	0.62	112
17.9	0.39	69.9

acrylate<sup>23</sup> (BMA:BA)  $\approx$  1:40, and methyl methacrylate:<sup>14</sup>methyl acrylate<sup>24</sup> (MMA:MA)  $\approx$  1:20. The values of  $k_p$  for AMS estimated in this work are about an order of magnitude lower than those previously estimated (at 60 °C:<sup>26,25</sup> and 47  $\text{dm}^3\cdot\text{mol}^{-1}\cdot\text{s}^{-1}$  4).

**Influence of Temperature on  $\langle k_p \rangle$ .** The Arrhenius plots for the average propagation rate coefficient at the different compositions are shown in Figure 5. From these plots the values of the average Arrhenius parameters,  $\langle E_a \rangle$  and  $\langle A \rangle$ , are calculated, where  $\langle k_p \rangle = \langle A \rangle \exp(-\langle E_a \rangle/RT)$ . The Arrhenius parameters for  $k_p^{\text{STY}}$  are found to be  $E_a = 33.6 \text{ kJ}\cdot\text{mol}^{-1}$  and  $A = 10^{7.88} \text{ dm}^3\cdot\text{mol}^{-1}\cdot\text{s}^{-1}$  which compare well with the IUPAC recommended values<sup>13</sup> of 32.5 and  $10^{7.63}$ , respectively. The Arrhenius parameters for the extrapolated values of  $k_p^{\text{AMS}}$ , from Table 1, are found to be  $E_a = 36.7 \text{ kJ}\cdot\text{mol}^{-1}$  and  $A = 10^{6.17} \text{ dm}^3\cdot\text{mol}^{-1}\cdot\text{s}^{-1}$ . The influences of  $f_{\text{AMS}}$  on  $\langle E_a \rangle$  and  $\log \langle A \rangle$  are shown in parts a and b of Figure 6, respectively. The closed circles, calculated directly from the plots in Figure 5, show some scatter. The primary reason this scatter is that the values of  $\langle k_p \rangle$  measured were only nominally at the same monomer feed composition; that is, each Arrhenius plot shown in Figure 5 actually contains data from slightly different monomer compositions. To overcome this, a linear regression of the  $\log \langle k_p \rangle$  vs  $f_{\text{AMS}}$  data (see Figure 4) at each temperature was used to obtain an interpolated value for  $\langle k_p \rangle$  at exactly the same  $f_{\text{AMS}}$ . The values of  $\langle E_a \rangle$  and  $\log \langle A \rangle$  calculated from the interpolated values are shown in Figure 6 as joined open squares, and show a strong linear trend. The data for Figure 6 are shown in Table 2.

The origin of the reduction in  $\langle k_p \rangle$  with decreasing  $f_{\text{AMS}}$  in this copolymerization is evident from the Arrhenius data;  $\langle E_a \rangle$  shows a small dependence on  $f_{\text{AMS}}$ , whereas  $\log \langle A \rangle$  shows a significantly larger dependence. The activation energy increases by about 3  $\text{kJ}\cdot\text{mol}^{-1}$  in going from pure STY to pure AMS, which corresponds to change of about a factor of 3 in  $k_p$  (at 50 °C). The



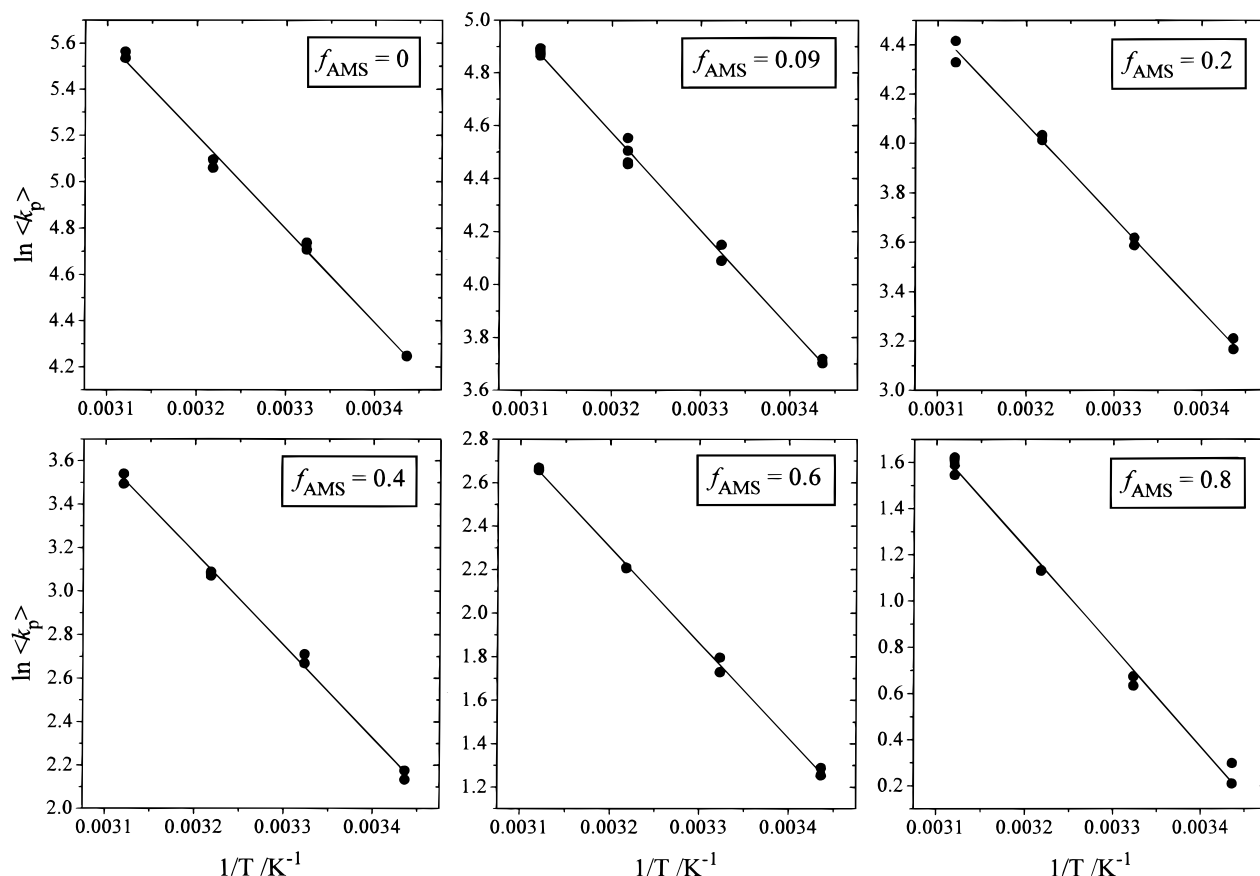


**Figure 5.** Arrhenius plots for  $\langle k_p \rangle$  at different nominal monomer feed compositions.

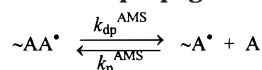
**Table 2.** Values of  $\langle E_a \rangle$  and  $\log \langle A \rangle$  at Various  $f_{\text{AMS}}$

$f_{\text{AMS}}$	experimental data <sup>a</sup>		interpolated data <sup>b</sup>	
	$\langle E_a \rangle^c$	$\log \langle A \rangle$	$\langle E_a \rangle^c$	$\log \langle A \rangle$
0	33.6	7.88		
0.1	30.6	7.11	32.9	7.49
0.2	31.4	7.02	33.3	7.34
0.4	35.4	7.29	34.2	7.05
0.6	36.5	7.09	35	6.76
0.8	35.8	6.52	35.9	6.46
1			36.7 <sup>d</sup>	6.17 <sup>d</sup>

<sup>a</sup> Determined from the slopes and intercepts in Figure 5; values of  $f_{\text{AMS}}$  for the experimental data are nominal. <sup>b</sup> Values of  $f_{\text{AMS}}$  for the interpolated data are exact. <sup>c</sup> kJ·mol<sup>-1</sup>. <sup>d</sup> Extrapolated values.

frequency factor of AMS is about 50 times lower than that for styrene, which corresponds to change of a factor of 50 in  $k_p$  (i.e., much greater than the change due to  $E_a$ ). Thus, the low propagation rate coefficient in  $\alpha$ -methylstyrene can be attributed primarily to the low-frequency factor. This observation can be understood in terms of the monomer and radical structure. The difference between STY and AMS is the presence of an  $\alpha$ -methyl group. Alkyl groups are known to exert relatively small electronic effects, which are reflected in the small, but still significant, difference in activation energies of the two homopropagation reactions. The  $\alpha$ -methyl group, however, is likely to affect the frequency factor,  $A$ , significantly, as suggested by recent theoretical studies,<sup>26–28</sup> where it was shown that the frequency factor is largely governed by torsional motions in the transition state of the propagation reaction—the most important of these is the rotation of the adding monomer about the forming C–C bond; see Figure 7. The introduction of an  $\alpha$ -methyl group will lead to a

**Scheme 1.** Depropagation in Case I: Only  $\alpha$ -Methylstyrene Sequences of Two ( $\sim$ AA $\cdot$ ) or Longer Can Depropagate



higher barrier to this rotation and a decrease in the frequency factor.

It has been well-known for many years that the primary cause of the low ceiling temperature in AMS originates in steric interactions in the formed polymer causing a low heat of polymerization,  $\Delta H$ ,<sup>2</sup> however, to our knowledge, steric factors in AMS homopolymerization have not been previously quantified in terms of Arrhenius parameters for the propagation reaction.

**Mechanistic Models For Predicting  $\langle k_p \rangle$ .** AMS homopolymerization exhibits a low ceiling temperature of 61 °C,<sup>2,3</sup> and copolymerizations involving AMS are known to be influenced by depropagation reactions.<sup>2,4–11</sup> The magnitude of the depropagation reaction is dependent on both the reaction temperature and the AMS concentration in the feed; therefore, any general copolymerization model for AMS needs to accommodate the depropagation reaction. In this paper, two different depropagation models are investigated (depropagation case I and depropagation case II) in addition to the terminal model. Lowry's<sup>29</sup> models for copolymerization with depropagation define a minimum number of consecutive AMS monomer units, preceded by a styrene unit, that need to be present on the radical endgroup to allow depropagation. In case I (see Scheme 1), only AMS sequences of two or longer can depropagate. In case II (Scheme 2), only AMS sequences of three or longer can depropagate.

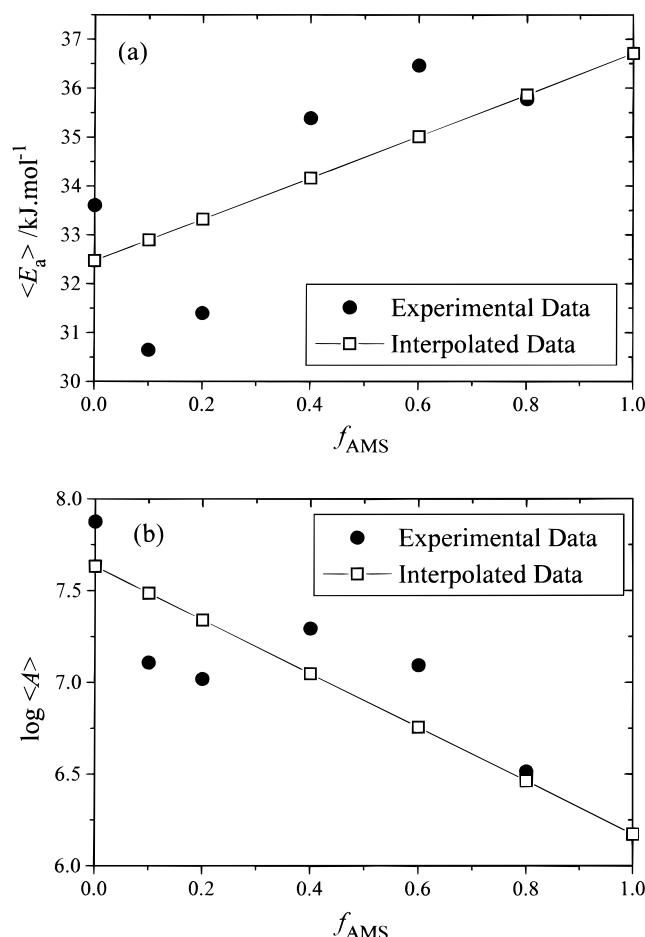


**Figure 6.** Dependence of (a)  $\langle E_a \rangle$  on  $f_{AMS}$ , and (b)  $\log \langle A \rangle$  on  $f_{AMS}$ . Closed circles correspond to values determined directly from Figure 5. Open squares are obtained if the  $\langle k_p \rangle$  vs  $f_{AMS}$  data are interpolated using a linear regression on  $\log \langle k_p \rangle$  (as in Figure 4), so that various temperatures are taken at exactly the same monomer feed composition.

Lowry<sup>29</sup> published expressions for the effect of depropagation on the polymer composition in a copolymerization for three cases, i.e., I, II, and III. Using Lowry's models, expressions for  $\langle k_p \rangle$  vs  $f_{AMS}$  for case I and case II were derived (case III is applicable when both monomers can depolymerize). The derivations are given in the Appendix.

The terminal model expression for  $\langle k_p \rangle$  is

$$\langle k_p \rangle = \frac{r_{STY}[STY]^2 + 2[AMS][STY] + r_{AMS}[AMS]^2}{([STY] + [AMS]) \left( \frac{r_{AMS}[AMS]}{k_p^{AMS}} + \frac{r_{STY}[STY]}{k_p^{STY}} \right)} \quad (5)$$

where  $r_{AMS}$  and  $r_{STY}$  are the monomer reactivity ratios,  $f_{AMS}$  and  $f_{STY}$  are the mole fractions of monomer in the feed, and  $k_p^{AMS}$  and  $k_p^{STY}$  are the homopropagation rate coefficients.

The expression for  $\langle k_p \rangle$  in depropagation case I is

$$\langle k_p \rangle = \frac{r_{STY}[STY]^2 + 2[AMS][STY] + r_{AMS}[AMS]^2 - \alpha r_{AMS}[AMS]/K}{([STY] + [AMS]) \left( \frac{r_{AMS}[AMS]}{k_p^{AMS}} + \frac{r_{STY}[STY]}{k_p^{STY}} \right)} \quad (6)$$

where  $K$  is the equilibrium constant for depropagation

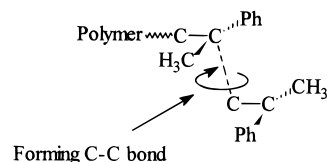


**Figure 7.** Rotation of the monomer around the forming C-C bond in the monomer addition step.

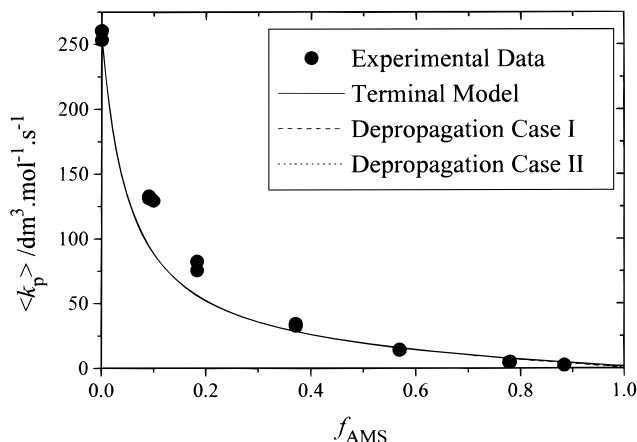
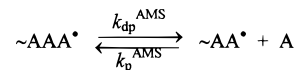


**Figure 8.** Comparison of terminal, depropagation case I, and depropagation case II models in their ability to describe  $\langle k_p \rangle$  vs  $f_{AMS}$  data measured by PLP at 47.4 °C. The model parameters used were  $r_{STY}^{STY} = 0.117$ ,  $r_{STY}^{STY} = 0.974$ ,  $k_p^{AMS} = 1.54 \text{ dm}^3 \cdot \text{mol}^{-1} \cdot \text{s}^{-1}$ ,  $k_p^{STY} = 257 \text{ dm}^3 \cdot \text{mol}^{-1} \cdot \text{s}^{-1}$ , and  $K = 0.204 \text{ L} \cdot \text{mol}^{-1}$ .

**Scheme 2. Depropagation in Case II: Only  $\alpha$ -Methylstyrene Sequences of Three ( $\sim AAA \cdot$ ) or Longer Can Depropagate**



( $= k_p^{AMS}/k_{dp}^{AMS}$ ) and  $\alpha$  is a parameter that varies between 0 and 1 (see the Appendix for definition eq A7). This expression is analogous to the one for the terminal model, eq 5.

The expression for  $\langle k_p \rangle$  in depropagation case II is

$$\langle k_p \rangle = \frac{r_{STY}[STY]^2 + 2[AMS][STY] + r_{AMS}[AMS]^2 - \delta r_{AMS}[AMS]/K}{([STY] + [AMS]) \left( \frac{r_{AMS}[AMS]}{k_p^{AMS}} + \frac{r_{STY}[STY]}{k_p^{STY}} \right)} \quad (7)$$

where  $K = k_p^{AMS}/k_{dp}^{AMS}$  and  $\delta$  is a parameter that varies between 0 and 1 (see the Appendix for definition eqs A20, A21, and A24). This expression is identical to eq 6 except that  $\delta$  has a more complex definition than  $\alpha$ .

In the model predictions, the monomer reactivity ratios used are as follows:  $\log r_{AMS} = 2.48 - 1094/T$ , and  $\log r_{STY} = 0.378 - 125/T$ ,<sup>4</sup> and the values for  $k_p^{STY}$  and  $k_p^{AMS}$  used are shown in Table 1. The equilibrium constant for depropagation,  $K$ , was calculated from the free energy of polymerization

$$\Delta G = \Delta H - T\Delta S = -RT \ln K \quad (8)$$

where  $\Delta H = -29.1 \text{ kJ} \cdot \text{mol}^{-1}$  and  $\Delta S = -104 \text{ J} \cdot \text{mol}^{-1} \cdot \text{K}^{-1}$  for AMS,<sup>3</sup>  $T$  is the temperature, and  $R$  is the universal gas constant ( $8.314 \text{ J} \cdot \text{mol}^{-1} \cdot \text{K}^{-1}$ ).

Figure 8 shows the experimental data along with the three model predictions. On this scale there is no

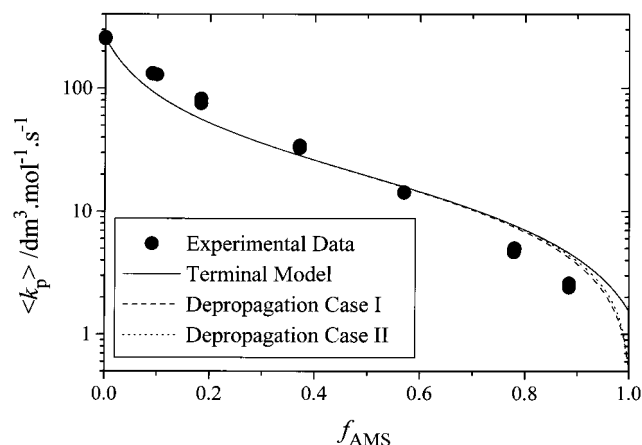


**Figure 9.** Replot of Figure 8 on a log  $\langle k_p \rangle$  scale to better show the differences between the models. Effects from the depropagation of AMS are negligible for  $f_{\text{AMS}} < 0.9$ .

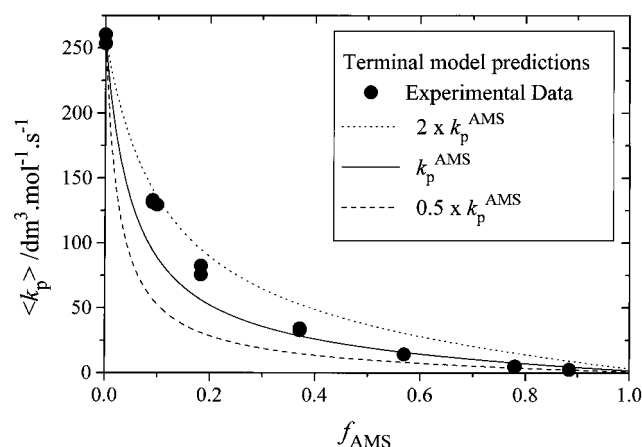


**Figure 10.** Dependence of  $\langle k_p \rangle$  on  $f_{\text{AMS}}$  measured by PLP at  $47.4^\circ\text{C}$ . The two broken lines show the sensitivity of the terminal model on  $k_p^{\text{AMS}}$  by varying it by a factor of 2.

apparent difference between the models. If  $\langle k_p \rangle$  is plotted on a log scale (Figure 9) the differences between the models can be highlighted. Figure 9 suggests that effects from depropagation are not expected to be seen until the mole fraction of AMS monomer is greater than 0.9; however, the difference is only truly significant once the styrene content approaches zero (i.e.  $f_{\text{AMS}} \approx 1$ ). As detailed earlier, the  $k_p$  for AMS was determined as an empirical value, and so it is not possible to ascertain with certainty if the depropagation models provide a better description of  $\langle k_p \rangle$ , since all three models describe the experimentally measured data equally well. Under such circumstances, we invoke Ockham's Razor<sup>30</sup> and utilize the terminal model because it is the simplest of the three. The terminal model prediction and the actual experimental data differ at most by a factor of 2. This agreement is seen as satisfactory since the  $\langle k_p \rangle$  values vary by 2 orders of magnitude over the feed compositional range, and the model contains no adjustable parameters.

Since the homopropagation rate coefficients for AMS were extrapolated, it seems appropriate to undertake a sensitivity analysis on these estimates and evaluate the influence of this parameter on the model prediction. A sensitivity analysis is shown in Figure 10, showing that varying  $k_p^{\text{AMS}}$  by a factor of 2 causes the terminal model fit to worsen. Therefore, it appears that the extrapolated values of  $k_p$  for AMS are of the right magnitude.

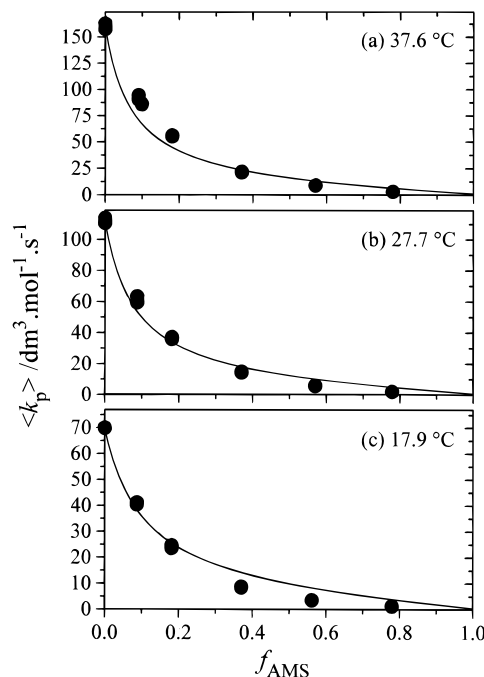


**Figure 11.** Dependence of  $\langle k_p \rangle$  on  $f_{\text{AMS}}$  measured by PLP at (a)  $37.6^\circ\text{C}$ , (b)  $27.7^\circ\text{C}$ , and (c)  $17.9^\circ\text{C}$ . Lines correspond to a terminal model prediction using (a)  $r_{\text{STY}} = 0.0910$ ,  $r_{\text{STY}} = 0.945$ ,  $k_p^{\text{AMS}} = 1.03 \text{ dm}^3 \cdot \text{mol}^{-1} \cdot \text{s}^{-1}$ , and  $k_p^{\text{STY}} = 160 \text{ dm}^3 \cdot \text{mol}^{-1} \cdot \text{s}^{-1}$ ; (b)  $r_{\text{STY}} = 0.0698$ ,  $r_{\text{STY}} = 0.919$ ,  $k_p^{\text{AMS}} = 0.620 \text{ dm}^3 \cdot \text{mol}^{-1} \cdot \text{s}^{-1}$ , and  $k_p^{\text{STY}} = 112 \text{ dm}^3 \cdot \text{mol}^{-1} \cdot \text{s}^{-1}$ ; and (c)  $r_{\text{STY}} = 0.0526$ ,  $r_{\text{STY}} = 0.890$ ,  $k_p^{\text{AMS}} = 0.387 \text{ dm}^3 \cdot \text{mol}^{-1} \cdot \text{s}^{-1}$ , and  $k_p^{\text{STY}} = 69.9 \text{ dm}^3 \cdot \text{mol}^{-1} \cdot \text{s}^{-1}$ .

The dependence of  $\langle k_p \rangle$  on  $f_{\text{AMS}}$ , for the temperatures  $37.6^\circ\text{C}$ ,  $27.7^\circ\text{C}$ , and  $17.9^\circ\text{C}$ , are shown in parts a–c of Figure 11 along with terminal model predictions. Generally, the terminal model for  $\langle k_p \rangle$  fits the data well for each temperature set, eliminating the need for more complicated models, such as the penultimate model, which introduces extra (unnecessary?) parameters; however, it is noteworthy that as the temperature is decreased, the terminal model prediction of the experimental data at  $f_{\text{AMS}} \sim 0.1$ – $0.2$  improves, whereas the prediction at  $f_{\text{AMS}} > 0.5$  becomes worse.

**Comments on the Applicability of the Implicit Penultimate Unit Effect Model to AMS–STY Copolymerization.** Fukuda et al.<sup>31–34</sup> have shown that, in general, copolymerization propagation kinetics are governed by a penultimate unit effect which affects radical reactivity, but not selectivity (also termed the implicit or restricted penultimate unit effect). Therefore, the penultimate unit model with the simplifying assumption,  $s_{\text{AMSSTY}} = r_{\text{AMS}}r_{\text{STY}}$ , was fitted to  $\langle k_p \rangle$  data. This simplifying assumption has often been used to reduce the model to only one adjustable parameter;<sup>31,35</sup> however, it is only valid if the penultimate unit effect is solely enthalpic in nature (theoretical predictions<sup>36</sup> suggest that entropic effects may also be significant).

Figure 12 shows a comparison of the penultimate unit effect model and the terminal model on the data at  $47.4^\circ\text{C}$  on a log  $\langle k_p \rangle$  scale. Surprisingly, although the penultimate unit effect model contains an extra (adjustable) parameter, it provides a slightly worse prediction than the terminal model when the same parameters are used.

**Meaning of the Extrapolated Value for  $\langle k_p \rangle$  of AMS.** Earlier it was stated that, due to depropagation effects, the extrapolated value of  $k_p$  for AMS may actually represent the effective value for  $k_p$  (i.e.,  $k_p^{\text{eff}}$ )

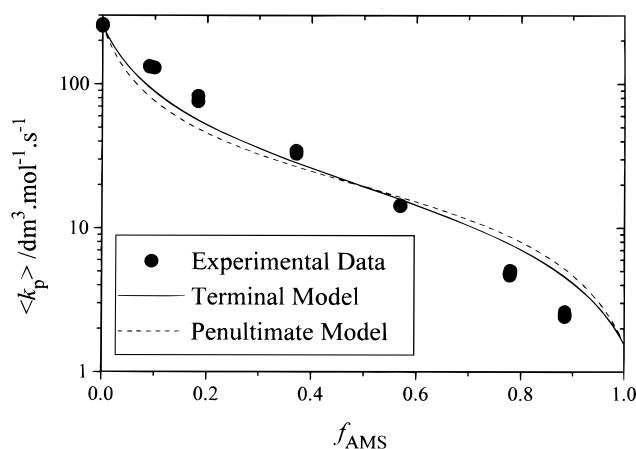
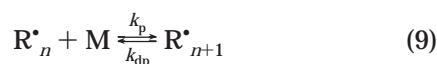


**Figure 12.** Comparison of penultimate unit and terminal models in their ability to describe  $\langle k_p \rangle$  vs  $f_{AMS}$  data measured by PLP at 47.4 °C. The model parameters used were  $r_{STY} = 0.117$ ,  $r_{STY} = 0.974$ ,  $k_p^{AMS} = 1.54 \text{ dm}^3 \cdot \text{mol}^{-1} \cdot \text{s}^{-1}$ ,  $k_p^{STY} = 257 \text{ dm}^3 \cdot \text{mol}^{-1} \cdot \text{s}^{-1}$ ,  $s_{AMS} = 1.57$ , and  $s_{STY} = 0.073$  (setting  $s_{STY} = r_{AMS} r_{STY}/s_{AMS}$ ).

and not the true forward propagation rate coefficient, thus it needs to be established which value is being estimated.

Under conditions where depolymerization is important, the propagation reaction should be written as an equilibrium reaction<sup>2</sup>



where  $k_{dp}$  is the rate coefficient for depolymerization. From eq 9, the overall rate of polymerization,  $R_p$ , can be written as

$$\begin{aligned} R_p &= k_p[M][R^*] - k_{dp}[R^*] \\ &= (k_p - k_{dp}/[M])[M][R^*] \\ &= k_p^{\text{eff}}[M][R^*] \end{aligned} \quad (10)$$

thus

$$\begin{aligned} k_p^{\text{eff}} &= k_p - k_{dp}/[M] \\ &= k_p (1 - 1/(K[M])) \end{aligned} \quad (11)$$

where  $K$  is the equilibrium constant for eq 9 (the value of  $K$  can be calculated from eq 8).

If the propagation rate coefficient for pure AMS was measured directly using PLP, then the value obtained from the MWD inflection point would in fact be  $k_p^{\text{eff}}$  and so the true  $k_p$  would need to be calculated using eq 11. In this work, however, the  $k_p$ s for pure AMS were extrapolated from copolymerization data over the range  $f_{AMS} = 0$  to  $\approx 0.8$ , and so it is not immediately clear if the extrapolated values reflect  $k_p^{\text{eff}}$  or the true  $k_p$  for AMS.

The meaning of the extrapolated values are established in two ways: (i) by considering the effect of depolymerization in the region of the measured data ( $f_{AMS} = 0$  to  $\approx 0.8$ ); (ii) by considering the values of the Arrhenius parameters. First, there is the effect of depolymerization: the two  $\langle k_p \rangle$  equations for case I and II depolymerization models (eqs 6 and 7) predict that effects from depolymerization do not manifest themselves until

$f_{AMS}$  is greater than about 0.9; see Figure 9. This suggests that all of the experimental data represent true values for  $\langle k_p \rangle$  and are not significantly influenced by AMS depolymerization. Thus, if one extrapolates to  $f_{AMS} = 1$  based on data that do not contain effects from depolymerization, it would also be expected that the extrapolated values would not contain effects from depolymerization, i.e., the extrapolation procedure obtains the true  $k_p$ s. Second, there is the Arrhenius parameters: if it is assumed that the extrapolated values represent the true  $k_p$  then the Arrhenius parameters obtained are those shown in Table 2 and Figure 6. It is clear from Figure 6 that there is a strong linear trend in the Arrhenius parameters over the whole range of  $f_{AMS}$ . If, alternately, it is assumed that the extrapolated values best represent  $k_p^{\text{eff}}$ , then the Arrhenius parameters for  $k_p$  of AMS calculated from the corresponding values of  $k_p$  (determined using eq 11) are  $E_a = 56.7 \text{ kJ} \cdot \text{mol}^{-1}$  and  $A = 10^{9.83} \text{ dm}^3 \cdot \text{mol}^{-1} \cdot \text{s}^{-1}$ . These values are significantly higher than those obtained for the copolymerizations and do not fit the trend of Figure 6.

As a result, it is felt that the extrapolated values best represent the true value of  $k_p$  for AMS and not  $k_p^{\text{eff}}$ .

**Effects of Depolymerization in AMS Homopolymerization.** From the Arrhenius parameters of  $k_p$  for AMS, Table 2, and the enthalpy and entropy of reaction, the Arrhenius parameters for the AMS depolymerization rate coefficient,  $k_{dp}$ , can be calculated:

$$K = \frac{k_p}{k_{dp}}$$

$$\ln K = \ln k_p - \ln k_{dp}$$

From eq 8 and the Arrhenius equation

$$-\frac{\Delta H}{RT} + \frac{\Delta S}{R} = \ln A_{k_p} - \frac{\Delta E_a^{k_p}}{RT} - \ln A_{k_{dp}} + \frac{\Delta E_a^{k_{dp}}}{RT}$$

grouping terms with and without  $T$  yields

$$\Delta H = \Delta E_a^{k_p} - \Delta E_a^{k_{dp}} \quad (12)$$

$$\Delta S = (\ln A_{k_p} - \ln A_{k_{dp}})R \quad (13)$$

Using eqs 12 and 13 the Arrhenius parameters for  $k_{dp}$  are calculated to be  $E_a^{k_{dp}} = 65.8 \text{ kJ} \cdot \text{mol}^{-1}$  and  $A_{k_{dp}} = 10^{11.6} \text{ dm}^3 \cdot \text{mol}^{-1} \cdot \text{s}^{-1}$ . The very high values for  $E_a^{k_{dp}}$  and  $A_{k_{dp}}$  (compared to those for  $k_p$ ) are in the order expected for unimolecular reactions. Figure 13 shows the Arrhenius plot for  $k_p$  and  $k_{dp}$  for AMS.

Using the Arrhenius parameters for  $k_p$  and  $k_{dp}$  and eq 11, it is possible to calculate the effective propagation rate coefficient,  $k_p^{\text{eff}}$ , as a function of temperature, Figure 14.  $k_{dp}$  is plotted as  $k_{dp}/[M]$  so as to match the dimensions in eq 11. It can be seen that as the temperature is increased both  $k_p$  and  $k_{dp}/[M]$  increase and become equal at about 60 °C; this corresponds to the ceiling temperature where  $k_p^{\text{eff}} = 0$ .  $k_p^{\text{eff}}$  has a maximum at about 40 °C, and so this temperature will give the maximum rate of polymerization for pure AMS (assuming the termination reactions are not strongly temperature dependent).

**Comparison of Propagation and Depolymerization Rate Coefficients.** The phenomenon of depolymerization is common to the majority of monomers.<sup>2</sup> Thus all polymerizations can be described by eq 9; however,



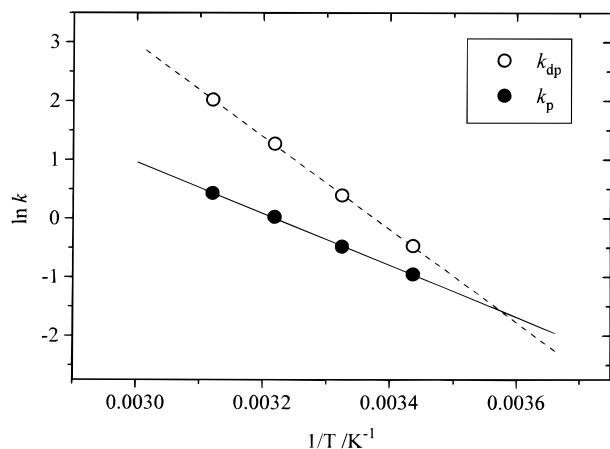


**Figure 13.** Arrhenius plots for  $k_p$  and  $k_{dp}$  in the homopolymerization of AMS.  $E_a^{k_p} = 36.7 \text{ kJ}\cdot\text{mol}^{-1}$ ,  $A_{k_p} = 10^{6.17} \text{ dm}^3\cdot\text{mol}^{-1}\cdot\text{s}^{-1}$ ,  $E_a^{k_{dp}} = 65.8 \text{ kJ}\cdot\text{mol}^{-1}$ , and  $A_{k_{dp}} = 10^{11.6} \text{ dm}^3\cdot\text{mol}^{-1}\cdot\text{s}^{-1}$ . Values of  $k_p$  determined from linear extrapolation of the  $\langle k_p \rangle$  vs  $f_{\text{AMS}}$  data;  $k_{dp}$  determined from the equilibrium constant,  $K$ .

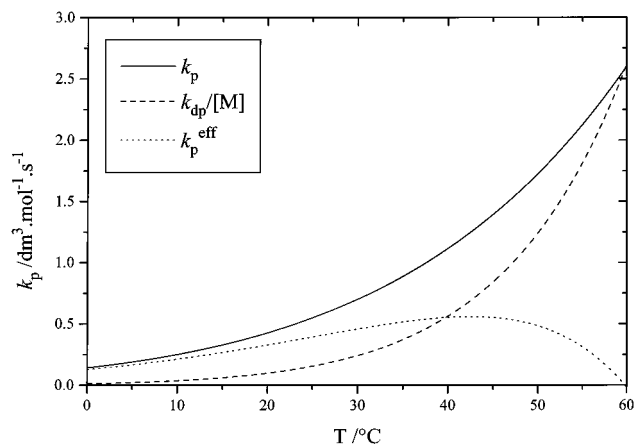


**Figure 14.** Dependence of  $k_p$ ,  $k_{dp}/[M]$ , and  $k_p^{\text{eff}}$  for the homopolymerization of AMS on temperature over the range 0–60 °C.  $k_p^{\text{eff}}$  has a maximum at approximately 40 °C.

monomers such as methyl methacrylate (MMA) and STY have very high ceiling temperatures, 220 and 300 °C, respectively (as compared to 61 °C for AMS), and so depropagation is not important under normal reaction conditions ( $T < 150$  °C).<sup>2</sup> The origin of the low ceiling temperature in AMS is 1,3 interactions in the product polymer causing a low  $\Delta H$ . This determines the equilibrium monomer concentration; however, the rate at which the polymerization proceeds to the equilibrium state is determined by both the  $k_p$  and  $k_{dp}$  values, which in turn depend on the respective Arrhenius parameters.

To compare the effect of depropagation in AMS, MMA, and STY homopolymerization, the respective equilibrium constants,  $K$ , depropagation rate coefficients,  $k_{dp}$ , and effective propagation rate coefficients,  $k_p^{\text{eff}}$ , were calculated from the free-energies of polymerization; see Table 3. For each monomer  $K$  is vastly different; however, it is interesting to note that the depropagation rates ( $k_{dp}/[M]$ ) for AMS and MMA at 50 °C are similar (only different by a factor of 2). Since  $k_p$  for MMA is 2 orders magnitude greater than  $k_{dp}/[M]$ ,  $k_p^{\text{eff}}$  is essentially the same as  $k_p$ , and depropagation has little influence on the overall reaction. On the other hand, in AMS polymerization the value of  $k_p$  is similar to  $k_{dp}/[M]$ , and so depropagation is important. In the polymerization of STY,  $k_{dp}/[M]$  is very low (7 orders of

**Table 3.** Effect of Depropagation on the Homopolymerizations of AMS, MMA, and STY at 50 °C

parameter	AMS <sup>a</sup>	MMA <sup>b</sup>	STY <sup>c</sup>
$\Delta H^d$	−29.1	−54	−73
$\Delta S^e$	−104	−127	−104
$K^f$	0.187	124	$2.33 \times 10^6$
$k_p^g$	1.73	649	237
$k_{dp}/[M]^g$	1.24	0.58	$1.20 \times 10^{-5}$
$k_p^{\text{eff } g}$	0.49	648	237

<sup>a</sup>  $\Delta H$  and  $\Delta S$  are from ref 3, and  $[M] = 7.44 \text{ mol}\cdot\text{L}^{-1}$ . <sup>b</sup>  $\Delta H$  and  $\Delta S$  are from ref 38,  $k_p = 10^{6.427} \exp(-22360/(RT))$ ,<sup>14</sup> and  $[M] = 9.0 \text{ mol}\cdot\text{L}^{-1}$ . <sup>c</sup>  $\Delta H$  and  $\Delta S$  are from ref 38,  $k_p = 10^{7.630} \exp(-32510/(RT))$ ,<sup>13</sup> and  $[M] = 8.44 \text{ mol}\cdot\text{L}^{-1}$ . <sup>d</sup>  $\text{kJ}\cdot\text{mol}^{-1}$ . <sup>e</sup>  $\text{J}\cdot\text{mol}^{-1}\cdot\text{K}^{-1}$ . <sup>f</sup>  $\text{L}\cdot\text{mol}^{-1}$ , calculated using eq 8. <sup>g</sup>  $\text{dm}^3\cdot\text{mol}^{-1}\cdot\text{s}^{-1}$ .

magnitude less than  $k_p$ ), and so effects from depropagation are negligible.

## Conclusions

The average propagation rate coefficient in the copolymerization decreases by about 2 orders of magnitude as the monomer composition is varied from pure styrene to pure  $\alpha$ -methylstyrene. This is due primarily to a much lower frequency factor for the propagation rate coefficient of AMS (causing a decrease by a factor of  $\sim 50$ ), since the activation energies for both monomers appear similar (causing a decrease by only a factor of  $\sim 3$ ). The copolymerization of styrene and AMS is one of the few monomer pairs whose  $\langle k_p \rangle$  can be adequately described by the terminal model, and this indicates that penultimate unit effects in this system may not be significant. Suitable conditions to measure the  $k_p$  of pure AMS by pulsed-laser polymerization were not found, and so the values were estimated by extrapolation of the  $\langle k_p \rangle$  data. From the estimated values of  $k_p$  for AMS, the Arrhenius parameters for the both the propagation and depropagation rate coefficients were calculated.

**Acknowledgment.** We would like to thank Dr. Hans Heuts and Prof. Bob Gilbert for useful discussions, and the Australian Research Council for funding. We thank Dr. Steve O'Donohue at Polymer Laboratories, U.K., for supplying the poly(AMS) SEC standards. D.K. would also like to thank the Australian Government for an Australian Postgraduate Award.

## Appendix

In the copolymerization of styrene and  $\alpha$ -methylstyrene, it is necessary to allow for the possibility of depolymerization of the  $\alpha$ -methylstyrene monomer addition. In this appendix, analytical expressions for the copolymer composition,  $F_A$ , and average propagation rate coefficient,  $\langle k_p \rangle$ , as a function of the monomer fraction in the comonomer mixture,  $f_A$ , are derived. The derivations for case I and case II are based on the reaction schemes suggested by Lowry.<sup>29</sup> In the derivations, S represents the monomer which does not depolymerize (styrene) and A represents the monomer which may depolymerize ( $\alpha$ -methylstyrene).

Derivations for the copolymer composition have been previously published by Lowry<sup>29</sup> and Wittmer,<sup>6,7</sup> but the expressions derived herein resemble the terminal model equation and so it is easy to see the effect of depropagation. During the course of this work, an expression for  $\langle k_p \rangle$  with depropagation was published by Martinet and Guillot;<sup>10</sup> however, they did not provide a detailed derivation and it is not obvious how to calculate the

parameter  $\sigma$  which they define. Also, Meackin<sup>37</sup> has derived expressions to simulate the dependence of the monomer concentrations on time for copolymerizations with depropagation.

**Depropagation Case I. Model.** The conditions of the model are as follows:

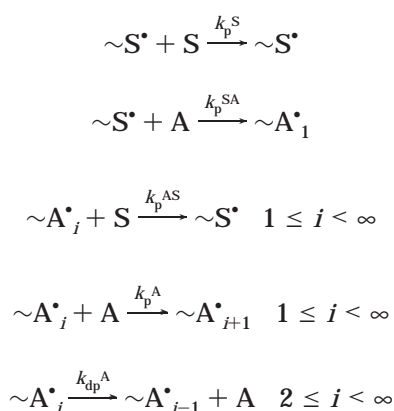
1. Monomer S has a negligible tendency to depolymerize regardless of the nature of the penultimate chain unit.

2. Monomer A has a negligible tendency to depolymerize only if it is attached to a monomer S unit.

3. Monomer A has an appreciable tendency to depolymerize if it is attached to another A monomer unit.

4. The rate of addition of a particular monomer to any given chain end or the rate of removal of a particular monomer from a given chain end is independent of the composition of the remainder of the chain.

This is represented in the following reaction scheme:



The symbol  $\sim A_i^\bullet$  represents an active chain end of  $i$  units of monomer A, immediately preceded by one or more units of monomer S. From this scheme, several steady-state expressions can be written as follows.

**Steady State in  $\sim S^\bullet$ :**

$$k_p^{AS} \sum_{i=1}^{\infty} [\sim A_i^\bullet][S] = k_p^{SA} [\sim S^\bullet][A] \quad (A1)$$

**Steady State in  $\sim A_1^\bullet$ .**

$$k_p^{SA} [\sim S^\bullet][A] + k_{dp}^A [\sim A_2^\bullet] = k_p^{AS} [\sim A_1^\bullet][S] + k_p^A [\sim A_1^\bullet][A] \quad (A2)$$

**Steady State in  $\sim A_i^\bullet$  ( $2 \leq i < \infty$ ).**

$$k_p^A [\sim A_{i-1}^\bullet][A] + k_{dp}^A [\sim A_{i+1}^\bullet] = k_p^{AS} [\sim A_i^\bullet][S] + k_p^A [\sim A_i^\bullet][A] + k_{dp}^A [\sim A_i^\bullet] \quad (A3)$$

**Define the following parameters.**

$$\begin{aligned}r_S &= \frac{k_p^S}{k_p^{SA}} \quad K = \frac{k_p^A}{k_{dp}^A} \\ r_A &= \frac{k_p^A}{k_p^{AS}} \quad \alpha = \frac{[\sim A_{i+1}^\bullet]}{[\sim A_i^\bullet]}\end{aligned}$$

**From the Steady-State Expressions.** From eq A1

$$\sum_{i=1}^{\infty} [\sim A_i^\bullet] = \frac{k_p^{SA} [\sim S^\bullet][A]}{k_p^{AS} [S]} \quad (A4)$$

also

$$\begin{aligned}\sum_{i=1}^{\infty} [\sim A_i^\bullet] &= [\sim A_1^\bullet] + [\sim A_2^\bullet] + [\sim A_3^\bullet] + [\sim A_4^\bullet] + \dots + [\sim A_n^\bullet] \\ &= [\sim A_1^\bullet] + \alpha [\sim A_1^\bullet] + \alpha^2 [\sim A_1^\bullet] + \alpha^3 [\sim A_1^\bullet] + \dots + \alpha^{n-1} [\sim A_1^\bullet] \\ &= [\sim A_1^\bullet] (1 + \alpha + \alpha^2 + \alpha^3 + \dots + \alpha^{n-1}) \\ &= [\sim A_1^\bullet] \left( \frac{1 - \alpha^n}{1 - \alpha} \right)\end{aligned}$$

in the limit as  $n \rightarrow \infty$ , and since  $0 < \alpha < 1$

$$\sum_{i=1}^{\infty} [\sim A_i^\bullet] = \frac{[\sim A_1^\bullet]}{1 - \alpha}$$

therefore

$$[\sim A_1^\bullet] = \frac{k_p^{SA} [\sim S^\bullet][A](1 - \alpha)}{k_p^{AS} [S]} \quad (A5)$$

From eq A2

$$\begin{aligned}k_p^{SA} [\sim S^\bullet][A] &= [\sim A_1^\bullet] (k_p^{AS} [S] + k_p^A [A] - k_{dp}^A \alpha) \\ [\sim A_1^\bullet] &= \frac{k_p^{SA} [\sim S^\bullet][A]}{k_p^{AS} [S] + k_p^A [A] - k_{dp}^A \alpha} \quad (A6)\end{aligned}$$

From eq A3

$$k_p^S \alpha^{-1} [\sim A_i^\bullet][A] + k_{dp}^A \alpha [\sim A_i^\bullet] = k_p^{AS} [\sim A_i^\bullet][S] + k_p^A [\sim A_i^\bullet][A] + k_{dp}^A [\sim A_i^\bullet]$$

Multiplying by  $(\alpha/k_{dp}^A)$  and rearranging gives

$$\alpha^2 - (1 + K[A] + K[S]/r_S)\alpha + K[A] = 0$$

In the solution of the quadratic equation in  $\alpha$ , only the negative sign in the numerator has physical significance (in order that  $0 < \alpha < 1$ ).

$$\begin{aligned}\alpha &= \frac{(1 + K[A] + K[S]/r_S) - \sqrt{(1 + K[A] + K[S]/r_S)^2 - 4K[A]}}{2} \quad (A7)\end{aligned}$$

This is also obtained by equating equations A5 and A6.

**Rate of Monomer Consumption.**

$$-\frac{d[S]}{dt} = k_p^S [\sim S^\bullet][S] + k_p^{AS} \sum_{i=1}^{\infty} [\sim A_i^\bullet][S]$$

using eq A1

$$-\frac{d[S]}{dt} = k_p^S[\sim S^*][S] + k_p^{SA}[\sim S^*][A] \quad (A8)$$

$$-\frac{d[A]}{dt} = k_p^{SA}[\sim S^*][A] + k_p^A \sum_{i=1}^{\infty} [\sim A^*]_i[A] - k_{dp}^A \sum_{i=2}^{\infty} [\sim A^*]_i$$

now

$$\begin{aligned} \sum_{i=2}^{\infty} [\sim A^*]_i &= \sum_{i=1}^{\infty} [\sim A^*]_i - [\sim A^*]_1 \\ -\frac{d[A]}{dt} &= k_p^{SA}[\sim S^*][A] + k_p^A \sum_{i=1}^{\infty} [\sim A^*]_i[A] - k_{dp}^A \sum_{i=1}^{\infty} [\sim A^*]_i + k_{dp}^A [\sim A^*]_1 \\ &= k_p^{SA}[\sim S^*][A] + (k_p^A[A] - k_{dp}^A) \sum_{i=1}^{\infty} [\sim A^*]_i + k_{dp}^A [\sim A^*]_1 \end{aligned}$$

using eqs A4 and A5

$$\begin{aligned} -\frac{d[A]}{dt} &= k_p^{SA}[\sim S^*][A] + \frac{(k_p^A[A] - k_{dp}^A)k_p^{SA}[\sim S^*][A]}{k_p^{AS}[S]} + \frac{k_{dp}^A k_p^{SA}[\sim S^*][A](1 - \alpha)}{k_p^{AS}[S]} \quad (A9) \end{aligned}$$

### Copolymer Composition.

$$\frac{d[A]}{d[S]} = \left( k_p^{SA}[\sim S^*][A] + \frac{(k_p^A[A] - k_{dp}^A)k_p^{SA}[\sim S^*][A]}{k_p^{AS}[S]} + \frac{k_{dp}^A k_p^{SA}[\sim S^*][A](1 - \alpha)}{k_p^{AS}[S]} \right) \left( k_p^S[\sim S^*][S] + k_p^{SA}[\sim S^*][A] \right)$$

by canceling  $[\sim S^*]$ , multiplying top and bottom by  $k_p^{AS}[S]/k_p^{SA}[A]$  and then  $1/k_p^A$ , then  $r_A[A]$  can be found.

$$\frac{d[A]}{d[S]} = \frac{[A][S] + r_A[A]^2 - \alpha r_A[A]/K}{r_S[S]^2 + [A][S]}$$

$$F_A = \frac{d[A]}{d[A] + d[S]} = \frac{[A][S] + r_A[A]^2 - \alpha r_A[A]/K}{r_S[S]^2 + 2[A][S] + r_A[A]^2 - \alpha r_A[A]/K} \quad (A10)$$

Cf. terminal model:

$$F_A = \frac{d[A]}{d[A] + d[S]} = \frac{[A][S] + r_A[A]^2}{r_S[S]^2 + 2[A][S] + r_A[A]^2}$$

Equation A10 is numerically equivalent to the equation derived by Lowry:<sup>23</sup>

$$F_A = \frac{d[A]}{d[A] + d[S]} = \frac{[A]}{r_S[S](1 - \alpha) + [A](2 - \alpha)}$$

This equation is simpler, but eq A10 shows closer resemblance to the terminal model expression.

### Average Propagation Rate Coefficient.

$$-\frac{d[M]}{dt} = \langle k_p \rangle [M][R^*]$$

$$-\frac{d[S]}{dt} - \frac{d[A]}{dt} = \langle k_p \rangle ([S] + [A])([\sim S^*] + \sum_{i=1}^{\infty} [\sim A^*]_i)$$

substituting eqs A4, A8, and A9 and canceling  $[\sim S^*]$

$$\begin{aligned} \langle k_p \rangle &= \left( k_p^S[S] + k_p^{SA}[A] + k_p^{SA}[A] + \frac{(k_p^A[A] - k_{dp}^A)k_p^{SA}[A]}{k_p^{AS}[S]} + \frac{k_{dp}^A k_p^{SA}[A](1 - \alpha)}{k_p^{AS}[S]} \right) \left( ([S] + [A]) \left( 1 + \frac{k_p^{SA}[A]}{k_p^{AS}[S]} \right) \right) \end{aligned}$$

multiplying top and bottom by  $k_p^{AS}[S]/k_p^{SA}[A]$  and then  $1/k_p^A$ , then  $r_A[A]$  can be found.

$$\langle k_p \rangle = \frac{r_S[S]^2 + 2[A][S] + r_A[A]^2 - \alpha r_A[A]/K}{([S] + [A]) \left( \frac{r_A[A]}{k_p^A} + \frac{r_S[S]}{k_p^S} \right)} \quad (A11)$$

Cf. terminal model:

$$\langle k_p \rangle = \frac{r_S[S]^2 + 2[A][S] + r_A[A]^2}{([S] + [A]) \left( \frac{r_A[A]}{k_p^A} + \frac{r_S[S]}{k_p^S} \right)}$$

**Depropagation Case II. Model.** The conditions of the model are as follows:

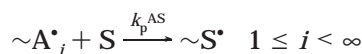
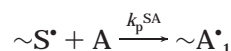
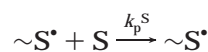
1. Monomer S has a negligible tendency to depolymerize regardless of the nature of the penultimate chain unit.

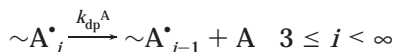
2. Monomer A has a negligible tendency to depolymerize only if it is attached to a monomer S unit or a single monomer A unit.

3. Monomer A has an appreciable tendency to depolymerize if it is attached to a sequence of two or more monomer A units.

4. The rate of addition of a particular monomer to any given chain end or the rate of removal of a particular monomer from a given chain end is independent of the composition of the remainder of the chain.

This is represented in the following reaction scheme:





**Steady State in  $\sim S^{\bullet}$ .**

$$k_p^{AS} \sum_{i=1}^{\infty} [\sim A^{\bullet}_i][S] = k_p^{SA} [\sim S^{\bullet}][A] \quad (A12)$$

**Steady State in  $\sim A^{\bullet}_1$ .**

$$k_p^{SA} [\sim S^{\bullet}][A] = k_p^{AS} [\sim A^{\bullet}_1][S] + k_p^A [\sim A^{\bullet}_1][A] \quad (A13)$$

**Steady State in  $\sim A^{\bullet}_2$ .**

$$k_p^A [\sim A^{\bullet}_1][A] + k_{dp}^A [\sim A^{\bullet}_3] = k_p^{AS} [\sim A^{\bullet}_2][S] + k_p^A [\sim A^{\bullet}_2][A] \quad (A14)$$

**Steady State in  $A^{\bullet}_i$  ( $3 \leq i < \infty$ ).**

$$k_p^A [\sim A^{\bullet}_{i-1}][A] + k_{dp}^A [\sim A^{\bullet}_{i+1}] = k_p^{AS} [\sim A^{\bullet}_i][S] + k_p^A [\sim A^{\bullet}_i][A] + k_{dp}^A [\sim A^{\bullet}_i] \quad (A15)$$

**Define the Following Parameters.**

$$r_S = \frac{k_p^S}{k_p^{SA}} \quad K = \frac{k_p^A}{k_{dp}^A} \quad \gamma = \frac{[\sim A^{\bullet}_1]}{[\sim A^{\bullet}_2]}$$

$$r_A = \frac{k_p^S}{k_p^{AS}} \quad \beta = \frac{[\sim A^{\bullet}_{i+1}]}{[\sim A^{\bullet}_i]}$$

**From the Steady-State Expressions.** From eq A12

$$\sum_{i=1}^{\infty} [\sim A^{\bullet}_i] = \frac{k_p^{SA} [\sim S^{\bullet}][A]}{k_p^{AS} [S]} \quad (A16)$$

also

$$\begin{aligned} \sum_{i=1}^{\infty} [\sim A^{\bullet}_i] &= [\sim A^{\bullet}_1] + [\sim A^{\bullet}_2] + [\sim A^{\bullet}_3] + [\sim A^{\bullet}_4] + \dots + [\sim A^{\bullet}_n] \\ &= \gamma [\sim A^{\bullet}_2] + [\sim A^{\bullet}_2] + \beta [\sim A^{\bullet}_2] + \beta^2 [\sim A^{\bullet}_2] + \dots + \beta^{n-2} [\sim A^{\bullet}_2] \\ &= [\sim A^{\bullet}_2] (\gamma + 1 + \beta + \beta^2 + \dots + \beta^{n-2}) \\ &= [\sim A^{\bullet}_2] \left( \gamma + \frac{1 - \beta^{n-2}}{1 - \beta} \right) \end{aligned}$$

in the limit as  $n \rightarrow \infty$ , and since  $0 < \beta < 1$

$$\sum_{i=1}^{\infty} [\sim A^{\bullet}_i] = [\sim A^{\bullet}_2] \left( \gamma + \frac{1}{1 - \beta} \right) \quad (A17)$$

therefore

$$[\sim S^{\bullet}] = \frac{k_p^{AS} [S]}{k_p^{SA} [A]} [\sim A^{\bullet}_2] \left( \gamma + \frac{1}{1 - \beta} \right) \quad (A18)$$

From eq A13

$$[\sim A^{\bullet}_1] (k_p^{AS} [S] + k_p^A [A]) = k_p^{SA} [\sim S^{\bullet}][A]$$

$$[\sim A^{\bullet}_1] = \frac{k_p^{SA} [\sim S^{\bullet}][A]}{k_p^{AS} [S] + k_p^A [A]} \quad (A19)$$

From eq A14

$$k_p^A \gamma [\sim A^{\bullet}_2][A] + k_{dp}^A \beta [\sim A^{\bullet}_2] = k_p^{AS} [\sim A^{\bullet}_2][S] + k_p^A [\sim A^{\bullet}_2][A]$$

$$\gamma = \frac{k_p^{AS} [S] + k_p^A [A] - k_{dp}^A \beta}{k_p^A [A]}$$

multiplying top and bottom by  $1/k_{dp}^A$

$$\gamma = \frac{K[S]/r_A + K[A] - \beta}{K[A]} \quad (A20)$$

From eq A15

$$k_p^S \beta^{-1} [\sim A^{\bullet}_i][A] + k_{dp}^A \beta [\sim A^{\bullet}_i] = k_p^{AS} [\sim A^{\bullet}_i][S] + k_p^A [\sim A^{\bullet}_i][A] + k_{dp}^A [\sim A^{\bullet}_i]$$

multiplying by  $(\beta/k_{dp}^A)$  and rearranging

$$\beta^2 - (1 + K[A] + K[S]/r_S) \beta + K[A] = 0$$

In the solution of the quadratic equation in  $\beta$ , only the negative sign in the numerator has physical significance (in order that  $0 < \beta < 1$ ).

$$\beta = \frac{(1 + K[A] + K[S]/r_S) - \sqrt{(1 + K[A] + K[S]/r_S)^2 - 4K[A]}}{2} \quad (A21)$$

It is noted that  $\beta$  has the same mathematical expression as  $\alpha$ , even though they have slightly different physical significances.

**Rate of Monomer Consumption.**

$$-\frac{d[S]}{dt} = k_p^S [\sim S^{\bullet}][S] + k_p^{AS} \sum_{i=1}^{\infty} [\sim A^{\bullet}_i][S]$$

using eqs A17 and A18

$$\begin{aligned} -\frac{d[S]}{dt} &= k_p^S \frac{k_p^{AS} [S]}{k_p^{SA} [A]} [\sim A^{\bullet}_2] \left( \gamma + \frac{1}{1 - \beta} \right) [S] + k_p^{AS} [\sim A^{\bullet}_2] \left( \gamma + \frac{1}{1 - \beta} \right) [S] \\ -\frac{d[S]}{dt} &= [\sim A^{\bullet}_2] k_p^{AS} [S] \left( \gamma + \frac{1}{1 - \beta} \right) \left( \frac{r_S [S]}{[A]} + 1 \right) \quad (A22) \end{aligned}$$

$$-\frac{d[A]}{dt} = k_p^{SA} [\sim S^{\bullet}][A] + k_p^A \sum_{i=1}^{\infty} [\sim A^{\bullet}_i][A] - k_{dp}^A \sum_{i=3}^{\infty} [\sim A^{\bullet}_i]$$

now

$$\sum_{i=3}^{\infty} [\sim A^{\bullet}_i] = \sum_{i=1}^{\infty} [\sim A^{\bullet}_i] - [\sim A^{\bullet}_1] - [\sim A^{\bullet}_2]$$



$$\begin{aligned}
-\frac{d[A]}{dt} &= k_p^{SA}[\sim S^*][A] + k_p^A \sum_{i=1}^{\infty} [\sim A^*]_i [A] - k_{dp}^A \sum_{i=1}^{\infty} [\sim A^*]_i + k_{dp}^A \gamma [\sim A^*]_2 + k_{dp}^A [\sim A^*]_2 \\
&= k_p^{SA}[\sim S^*][A] + (k_p^A[A] - k_{dp}^A) \sum_{i=1}^{\infty} [\sim A^*]_i + k_{dp}^A [\sim A^*]_2 (\gamma + 1)
\end{aligned}$$

using eqs A17 and A18

$$-\frac{d[A]}{dt} = [\sim A^*]_2 \left( \gamma + \frac{1}{1-\beta} \right) (k_p^{AS}[S] + k_p^A[A] - k_{dp}^A) + k_{dp}^A [\sim A^*]_2 (\gamma + 1) \quad (A23)$$

### Copolymer Composition.

$$\frac{d[A]}{d[S]} = \frac{[\sim A^*]_2 \left( \gamma + \frac{1}{1-\beta} \right) (k_p^{AS}[S] + k_p^A[A] - k_{dp}^A) + k_{dp}^A [\sim A^*]_2 (\gamma + 1)}{[\sim A^*]_2 k_p^{AS}[S] \left( \gamma + \frac{1}{1-\beta} \right) \left( \frac{r_S[S]}{[A]} + 1 \right)}$$

by canceling  $[\sim A^*]_2$ , and multiplying top and bottom by  $([A]/k_p^{AS})(\gamma + 1/(1-\beta))^{-1}$

$$\frac{d[A]}{d[S]} = \frac{[A][S] + r_A[A]^2 - \delta r_A[A]/K}{r_S[S]^2 + [A][S]}$$

$$\delta = 1 - (\gamma + 1) \left( \gamma + \frac{1}{1-\beta} \right)^{-1} \quad (A24)$$

$$F_A = \frac{d[A]}{d[A] + d[S]} = \frac{[A][S] + r_A[A]^2 - \delta r_A[A]/K}{r_S[S]^2 + 2[A][S] + r_A[A]^2 - \delta r_A[A]/K} \quad (A25)$$

Cf. terminal model

$$F_A = \frac{d[A]}{d[A] + d[S]} = \frac{[A][S] + r_A[A]^2}{r_S[S]^2 + 2[A][S] + r_A[A]^2}$$

Equation A25 is numerically equivalent to the equation derived by Lowry:<sup>23</sup>

$$F_A = \frac{d[A]}{d[A] + d[S]} = \frac{\beta\gamma - 1 + 1/(1-\beta)^2}{\left( \frac{r_S[S]}{[A]} + 1 \right) \left( \beta\gamma + \frac{\beta}{1-\beta} \right) + \beta\gamma - 1 + \frac{1}{(1-\beta)^2}}$$

This equation is of similar complexity, but eq A25 shows closer resemblance to the terminal model expression.

### Average Propagation Rate Coefficient.

$$-\frac{d[M]}{dt} = \langle k_p \rangle [M][R^*]$$

$$-\frac{d[S]}{dt} - \frac{d[A]}{dt} = \langle k_p \rangle ([S] + [A]) ([\sim S^*] + \sum_{i=1}^{\infty} [\sim A^*]_i)$$

substituting eqs A17, A22, and A23, and canceling  $[\sim A^*]_2$

$$\begin{aligned}
\langle k_p \rangle &= k_p^{AS}[S] \left( \gamma + \frac{1}{1-\beta} \right) \left( \frac{r_S[S]}{[A]} + 1 \right) + \left( \gamma + \frac{1}{1-\beta} \right) (k_p^{AS}[S] + k_p^A[A] - k_{dp}^A) + k_{dp}^A (\gamma + 1) \left( ([S] + [A]) \left( \frac{k_p^{AS}[S]}{k_p^{SA}[A]} \left( \gamma + \frac{1}{1-\beta} \right) + \left( \gamma + \frac{1}{1-\beta} \right) \right) \right)
\end{aligned}$$

multiplying top and bottom by  $([A]/k_p^{AS})(\gamma + 1/(1-\beta))^{-1}$

$$\langle k_p \rangle = \frac{r_S[S]^2 + 2[A][S] + r_A[A]^2 - \delta r_A[A]/K}{([S] + [A]) \left( \frac{r_A[A]}{k_p^A} + \frac{r_S[S]}{k_p^S} \right)} \quad (A26)$$

Cf. terminal model

$$\langle k_p \rangle = \frac{r_S[S]^2 + 2[A][S] + r_A[A]^2}{([S] + [A]) \left( \frac{r_A[A]}{k_p^A} + \frac{r_S[S]}{k_p^S} \right)}$$

**Using the Models.** It is usual to plot  $\langle k_p \rangle$  against the mole fraction of one of the monomers,  $f_A$ . The models for  $\langle k_p \rangle$ , however, are in terms of monomer concentrations. To convert mole fractions to monomer concentrations the following relationships are used:

$$f_S = 1 - f_A$$

$$[A] = 1000 \frac{f_A}{f_A m_A / d_A + f_S m_S / d_S}$$

$$[S] = 1000 \frac{f_S}{f_A m_A / d_A + f_S m_S / d_S}$$

Here  $d_A$ ,  $m_A$ ,  $d_S$  and  $m_S$  are the densities ( $\text{g}\cdot\text{cm}^{-3}$ ) and molecular weights ( $\text{g}\cdot\text{mol}^{-1}$ ) for monomers A and S, respectively.

**Supporting Information Available:** Tables giving the experimental conditions and results of the pulsed-laser polymerization of AMS and STY over the temperature range 17.9–47.4 °C (4 pages). Ordering and Internet access information is given on any current masthead page.

### References and Notes

- (1) Kukulj, D.; Davis, T. P.; Gilbert, R. G. *Macromolecules* **1998**, *31*, 994.
- (2) See, for example: Odian, G. *Principles of Polymerization*, 3rd ed.; Wiley-Interscience: New York, 1991.
- (3) McCormick, H. W. *J. Polym. Sci.* **1957**, *25*, 488.
- (4) Fischer, J. P. *Makromol. Chem.* **1972**, *155*, 211.
- (5) O'Driscoll, K. F.; Gasparro, F. P. *J. Macromol. Sci.-Chem.* **1967**, *A1*, 643.
- (6) Wittmer, P. *Adv. Chem. Ser.* **1971**, *99*, 140.
- (7) Wittmer, P. *Makromol. Chem.* **1976**, *177*, 997.
- (8) Johnston, H. K.; Rudin, A. *J. Paint Technol.* **1970**, *42*, 435.
- (9) O'Driscoll, K. F.; Dickson, J. R. *J. Macromol. Sci.-Chem.* **1968**, *A2*, 449.
- (10) Martinet, F.; Guillot, J. *J. Appl. Polym. Sci.* **1997**, *65*, 2297.
- (11) Kang, B. K.; O'Driscoll, K. F. *Macromolecules* **1974**, *7*, 886.
- (12) For recent reviews of the PLP/MWD technique see: (a) Van Herk, A. M. *J. Macromol. Sci.-Rev. Macromol. Chem. Phys.* **1997**, *C37*, 663. (b) Coote, M. L.; Zammit, M. D.; Davis, T. P. *Trends Polym. Sci.* **1996**, *4*, 189. (c) Davis, T. P. *J. Photochem. Photobiol., A* **1994**, *77*, 1.
- (13) Buback, M.; Gilbert, R. G.; Hutchinson, R. A.; Klumperman, B.; Kuchta, F.-D.; Manders, B. G.; O'Driscoll, K. F.; Russell, G. T.; Schweer, J. *Macromol. Chem. Phys.* **1995**, *196*, 3267.

- (14) Beuermann, S.; Buback, M.; Davis, T. P.; Gilbert, R. G.; Hutchinson, R. A.; Olaj, O. F.; Russell, G. T.; Schweer, J.; van Herk, A. M. *Macromol. Chem. Phys.* **1997**, *198*, 1545.
- (15) Davis, T. P.; O'Driscoll, K. F.; Piton, M. C.; Winnik, M. A. *Macromolecules* **1989**, *22*, 2785.
- (16) Coulter, K. E.; H., K.; Hiscock, B. F. in *Vinyl and Diene Monomers*; Leonard, E. C., Ed.; Wiley-Interscience: New York, 1971; Vol. 2.
- (17) Weast, R. C. *CRC Handbook of Chemistry and Physics*, 69th ed.; Weast, R. C., Ed.; CRC Press: Boca Raton, FL, 1989.
- (18) Davis, T. P.; O'Driscoll, K. F.; Piton, M. C.; Winnik, M. A. *J. Polym. Sci., Polym. Lett. Ed.* **1989**, *27*, 181.
- (19) Coote, M. L.; Zammit, M. D.; Willett, G. D.; Davis, T. P. *Macromolecules* **1997**, *30*, 8182.
- (20) Hutchinson, R. A.; McMinn, J. H.; Paquet, D. A.; Beuermann, S.; Jackson, C. *Ind. Eng. Chem. Res.* **1997**, *36*, 1103.
- (21) Hutchinson, R. A.; Aronson, M. T.; Richards, J. R. *Macromolecules* **1993**, *26*, 6410.
- (22) Hutchinson, R. A.; Paquet, D. A.; McMinn, J. H.; Beuermann, S.; Fuller, R. E.; Jackson, C. *DEHEMA Monogr.* **1995**, *131*, 467.
- (23) Beuermann, S.; Paquet, D. A.; McMinn, J. H.; Hutchinson, R. A. *Macromolecules* **1996**, *29*, 4206.
- (24) de Kock, J. B. L. *PLP of MA*; de Kock, J. B. L., Ed.; Eindhoven University of Technology: Eindhoven, The Netherlands, 1994.
- (25) Kang, B. K.; O'Driscoll, K. F.; Howell, J. A. *J. Polym. Sci., Part A-1* **1972**, *10*, 2349.
- (26) Heuts, J. P. A.; Gilbert, R. G.; Radom, L. *Macromolecules* **1995**, *28*, 8771.
- (27) Heuts, J. P. A.; Sudarko; Gilbert, R. G. *Macromol. Symp.* **1996**, *111*, 147.
- (28) Heuts, J. P. A.; Gilbert, R. G.; Radom, L. *J. Phys. Chem.* **1996**, *100*, 18997.
- (29) Lowry, G. G. *J. Polym. Sci.* **1960**, *42*, 463.
- (30) (a) Ockham's Razor: "entities are not to be multiplied beyond necessity"; William of Ockham, 1300–1349. (b) The application of Ockham's razor to copolymerization model discrimination was first invoked by Moad et al.<sup>30c</sup> in a paper cautioning that the difficulty in observing penultimate unit effects does not necessarily indicate their absence. The same comments are relevant in this work. (c) Moad, G.; Solomon, D. H.; Spurling, T. H.; Stone, R. A. *Macromolecules* **1989**, *22*, 1145.
- (31) Fukuda, T.; Kubo, K.; Ma, Y.-D. *Prog. Polym. Sci.* **1992**, *17*, 875.
- (32) Fukuda, T.; Ma, Y.-D.; Inagaki, H. *Macromolecules* **1985**, *18*, 17.
- (33) Fukuda, T.; Ma, Y.-D.; Inagaki, H. *Makromol. Chem., Rapid Commun.* **1987**, *8*, 495.
- (34) Fukuda, T.; Ma, Y.-D.; Kubo, K.; Inagaki, H. *Macromolecules* **1991**, *24*, 370.
- (35) Davis, T. P.; O'Driscoll, K. F.; Piton, M. C.; Winnik, M. A. *Macromolecules* **1990**, *23*, 2113.
- (36) Heuts, J. P. A.; Gilbert, R. G.; Maxwell, I. A. *Macromolecules* **1997**, *30*, 726.
- (37) Meakin, P. *Macromolecules* **1983**, *16*, 1661.
- (38) Brandrup, J.; Immergut, E. H. In *Polymer Handbook*, 3rd ed.; Brandrup, J., Immergut, E. H., Eds.; Wiley-Interscience: New York, 1989.

MA980028J